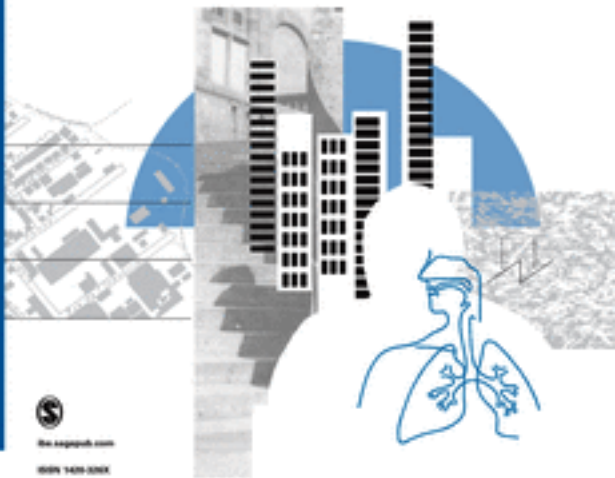


Indoor and Built Environment

Originally published as the
Journal of the International Society of the Built Environment

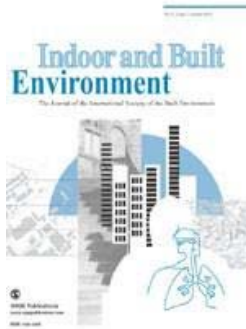


dx.doi.org/10.1080/14487013.2015.1028308

ISSN 1448-301X

Cart (0)

Find My Rep | Login | Contact | Your cart is empty.

[Disciplines](#) | [Products](#) | [Resources](#) | [About](#)Search: keyword, t
Search[Journal](#) > [Environmental Health](#)[Back to journals](#)

Indoor and Built Environment

2013 Impact Factor: 1.716**2013 Ranking**75/162 in Public, Environmental & Occupational Health (SCI) | 11/58 in Construction & Building Technology | 22/46 in Engineering, Environmental

Source: 2013 Journal Citation Reports® (Thomson Reuters, 2014)

Share

Editor-in-Chief[Prof Chuck Yu](#) President and Executive Director, EnviroAct Consultants, ISBE Ltd., UK**Deputy Editors**[Dr Zhishi Guo](#) US EPA, USA[Dr. Marcella Ucci](#) University College London, UK**Assistant Editor**[Dr Yan Cheng](#) Xi'an Jiaotong University, China

eISSN: 14230070 | ISSN: 1420326X | Current volume: 24 | Current issue: 1 | Frequency: 8 Times/Year

[Print flyer](#) [Recommend to Library](#)

- [Description](#)
- [Aims and Scope](#)
- [Editorial Board](#)
- [Abstracting / Indexing](#)
- [Submission Guidelines](#)

REGIONAL EDITOR: NORTH AMERICA

[Prof Karen Bartlett](#) University of British Columbia (UBC), Canada[Prof. Charlene W. Bayer](#) Georgia Institute of Technology and US GBC, USA[Prof Jong Jin Kim](#) The University of Michigan, USA[Dr. Josephine Lau](#) University of Nebraska - Lincoln, USA

REGIONAL EDITOR: EUROPE

Search on SAGE Journals

submit

[Read Online](#)[Sample Issues](#)[Current Issue](#)[Email Alert](#)[Permissions](#)[Foreign rights](#)[Reprints and sponsorship](#)[Advertising](#)[Subscribe](#)

[Dr Derrick Crump](#) Institute of Environment and Health, Cranfield University, UK

[Prof Bob Giddings](#) Northumbria University, UK

[Prof Beata Gutarowska](#) Technical University of Lodz, Institute of Technology Fermentation and Microbiology, Poland

[Prof. Phil Jones](#) University of Cardiff, Wales

[Dr Stylianos Kephelopoulos](#) European Commission Joint Research Centre (ISPRA), Italy

[Dr. Pawel Wargocki](#) Technical University of Denmark, Denmark

REGIONAL EDITOR: CHINA

[Prof. Zhaolin Gu](#) Xian Jiaotong University, China

[Prof. Angui Li](#) Xi'an University of Architecture & Technology, China

[Prof Xianting Li](#) Tsinghua University, China

[Prof. Wei Xu](#) China Academy of Building Research, China

REGIONAL EDITOR: HONG KONG

[Prof. Albert Chan](#) The Hong Kong Polytechnic University, Hong Kong

[Prof Christopher Chao](#) The Hong Kong University of Science and Technology, Hong Kong

REGIONAL EDITOR: KOREA

[Prof. Jeong Tai Kim](#) CSHeB, Kyung Hee University, Korea

REGIONAL EDITOR: JAPAN

[Dr Kazuhide Ito](#) Kyushu University, Japan

REGIONAL EDITOR: AUSTRALIA

[Dr Stephen Brown](#) CSIRO, Australia

REGIONAL EDITOR: SOUTH EAST ASIA

[Prof. Chandra Sekhar](#) National University of Singapore, Singapore

[Dr Yat Yau](#) University of Malaya, Malaysia

REGIONAL EDITOR: GLOBAL

[Prof Helena
Yoon](#)

The UN-Habitat Korea Coalition and Yonsei-SERI EU
Center, Yonsei University, Korea

EDITORIAL BOARD

[Prof Dariush Azimi](#)

Ashford University, USA

[Prof Julie Bregulla](#)

BRE, UK

[Dr. Christine
Däumling](#)

Federal Environment Agency, AgBB, Germany

[Prof Qi-Hong Deng](#)

Central South University, China

[Dr Caroline Hachem](#)

Concordia University, Canada

[Prof. Paul Harrison](#)

PTCH Consultancy Ltd., UK

[Prof. Sture
Holmberg](#)

Royal Institute of Technology (KTH), Sweden

[Dr Wolfgang Horn](#)

BAM, Germany

[Dr Alvin Lai](#)

City University of Hong Kong, Hong Kong

[Dr. Berangere
Lartigue](#)

Paul Sabatier University, France

[Prof Ching Chang
Lee](#)

National Cheng Kung University, Taiwan

[Dr Young Lee](#)

Michigan State University, USA

[Dr Danny Li](#)

City University of Hong Kong, Hong Kong

[Dr. Xiaoyu Liu](#)

US EPA, USA

[Professor Vivian
Loftness](#)

Carnegie Mellon University, USA

[Dr. Ahmed Megri](#)

North Carolina A&T State University, USA

[Prof Lidia Morawska](#)

Queensland University of Technology, Australia

[Prof Fergus Nicol](#)

Oxford Brookes University, UK

[Prof Jianlei Niu](#)

The Hong Kong Polytechnic University, Hong Kong

[Prof. Catherine
Noakes](#)

University of Leeds, UK

[Prof. Shin-ichi
Tanabe](#)

Waseda University, Japan

[Prof. Joost van Hoof](#)

Fontys University of Applied Sciences, The
Netherlands

[Dr Jörn von Grabe](#)

Timber Engineering and Building Construction, TU
Munchen, Germany

[Dr. Xin Wang](#)

Tsinghua University, China

[Dr. Doyun Won](#)

National Research Council, Canada

[Dr Ling Tim Wong](#)

The Hong Kong Polytechnic University, Hong Kong

[Prof Runming Yao](#)

University of Reading, UK

[Dr John Zhai](#)

University of Colorado at Boulder, USA

[Prof. Lizhi Zhang](#)

South China University of Technology, China.

Browse

Books

Journals

Digital Library Products

Digital Solutions for your

Course

Resources For

Instructors

Societies

Book Authors/Editors

Journal Authors/Editors

/Reviewers

Students

Researchers

Librarians

About

About SAGE

Contact

Find My Rep

News

My Account

Careers

Social

[Facebook](#)[Twitter](#)[Google](#)

[Plus](#)[Mail](#)

You are in: **North**

America

[Change location](#)



FREE Online trial to SAGE Materials Science, Engineering & Computing journals >

[Sign In](#) | [My Tools](#) | [Contact Us](#) | [HELP](#)

[Search all journals](#)



[Advanced Search](#)

[Search History](#)

[Browse Journals](#)

Impact Factor: 1.716 | **Ranking:** Construction & Building Technology 11 out of 58 | Engineering, Environmental 22 out of 46 | Public, Environmental & Occupational Health (SCI) 75 out of 162

Source: 2013 Journal Citation Reports® (Thomson Reuters, 2014)

OnlineFirst

Last updated June 1, 2015

Indoor and Built Environment offers OnlineFirst, by which forthcoming articles are published online before they are scheduled to appear in print. More details, including how to cite OnlineFirst articles, can be found on the [OnlineFirst Fact Sheet](#).

Receive updates by email: [\[Sign up for eTOCs\]](#)

To see an article, click its [PDF] link. **To add articles to your marked citations,** check the boxes to the left of the titles you want, and click the 'Add to Marked Citations' button.

To see one abstract at a time, click its [Abstract] link.

June 1, 2015

Original Paper:

Xiaodong Xuan

Effectiveness of indoor environment quality in LEED-certified healthcare settings

Indoor and Built Environment 1420326X15587564, first published on June 1, 2015 as doi:10.1177/1420326X15587564

[Abstract](#) [Full Text \(PDF\)](#) [References](#)

Original Paper:

Atwar Qadir, Muhammad Tufail, Anwar Qadir, and Mayeen Uddin Khandaker

Indoor radon concentration in hydrocarbon and non-hydrocarbon pertaining areas across the Main Boundary Thrust in Attock district of Pakistan

Indoor and Built Environment 1420326X15588213, first published on June 1, 2015 as doi:10.1177/1420326X15588213

[Abstract](#) [Full Text \(PDF\)](#) [References](#)

Original Paper:

Ningbo Zhang, Yanming Kang, Ke Zhong, and Jiaping Liu

Indoor environmental quality of high occupancy dormitory buildings in winter in Shanghai, China

Indoor and Built Environment 1420326X15586443, first published on June 1, 2015 as doi:10.1177/1420326X15586443

[Abstract](#) [Full Text \(PDF\)](#) [References](#)

Original Paper:

Youngju Na, Shraddha Palikhe, Chaeyeon Lim, and Sunkuk Kim

Health performance and cost management model for sustainable healthy buildings

Indoor and Built Environment 1420326X15586585, first published on June 1, 2015 as doi:10.1177/1420326X15586585

[Abstract](#) [Full Text \(PDF\)](#) [References](#)

Original Paper:

B. Kucukomeroglu, E. Ozturk, N. Damla, N. Celik, S. Uzun Duran, U. Cevik, H. Taskin, and N. Albayrak

Indoor radon and gamma spectrometric measurements for the Erzincan Basin on North Anatolian Fault Zone, Turkey

Indoor and Built Environment 1420326X15588329, first published on June 1, 2015 as doi:10.1177/1420326X15588329

[Abstract](#) [Full Text \(PDF\)](#)  [References](#)

May 31, 2015

Original Paper:

Nikola Unković, Milica Ljaljević Grbić, Gordana Subakov-Simić, Miloš Stupar, Jelena Vukojević, Aleksa Jelikić, and Dragan Stanojević

Biodeteriogenic and toxigenic agents on 17th century mural paintings and façade of the old church of the Holy Ascension (Veliki Krčimir, Serbia)

Indoor and Built Environment 1420326X15587178, first published on May 22, 2015 as doi:10.1177/1420326X15587178

[Abstract](#) [Full Text \(PDF\)](#)  [References](#)

Original Paper:

Carla A. Ramos, Carla Viegas, Sandra Cabo Verde, Humbert T. Wolterbeek, and Susana M. Almeida

Characterizing the fungal and bacterial microflora and concentrations in fitness centres

Indoor and Built Environment 1420326X15587954, first published on May 31, 2015 as doi:10.1177/1420326X15587954

[Abstract](#) [Full Text \(PDF\)](#)  [References](#)

Original Paper:

Tafeng Hu, Junji Cao, Shuncheng Lee, Kinfa Ho, Xuxiang Li, Suixin Liu, and Ji Chen

Physicochemical characteristics of indoor PM_{2.5} with combustion of dried yak dung as biofuel in Tibetan Plateau, China

Indoor and Built Environment 1420326X15586584, first published on May 31, 2015 as doi:10.1177/1420326X15586584

[Abstract](#) [Full Text \(PDF\)](#)  [References](#)

Original Paper:

Valerio R.M. Lo Verso, Federica Caffaro, and Chiara Aghemo

Luminous environment in healthcare buildings for user satisfaction and comfort: an objective and subjective field study

Indoor and Built Environment 1420326X15588337, first published on May 31, 2015 as doi:10.1177/1420326X15588337

[Abstract](#) [Full Text \(PDF\)](#)  [References](#)

May 25, 2015

Editorial:

Pawel Wargocki

What are indoor air quality priorities for energy-efficient buildings?

Indoor and Built Environment 1420326X15587824, first published on May 25, 2015 as doi:10.1177/1420326X15587824

[Full Text \(PDF\)](#) 

May 22, 2015

Original Paper:

D.H.W. Li, C. Li, S.W. Lou, E.K.W. Tsang, and J.C. Lam

Analysis of vertical sky components under various CIE standard general skies

Indoor and Built Environment 1420326X15587128, first published on May 22, 2015 as doi:10.1177/1420326X15587128

[Abstract](#) [Full Text \(PDF\)](#)  [References](#)

Original Paper:

Bo Yang, Weixing Yuan, Xiaohan He, and Kexian Ren

Air dehumidification by hollow fibre membrane with chilled water for spacecraft applications

Indoor and Built Environment 1420326X15587127, first published on May 22, 2015 as doi:10.1177/1420326X15587127

[Abstract](#) [Full Text \(PDF\)](#)  [References](#)

May 20, 2015

Original Article:

Xilian Luo, Zhaolin Gu, Chuck Yu, Tao Ma, and Kiwamu Kase

Efficacy of an air curtain system for local pit environmental control for relic preservation in archaeology museums

Indoor and Built Environment 1420326X15585327, first published on May 20, 2015 as doi:10.1177/1420326X15585327

[Abstract](#) [Full Text \(PDF\)](#)  [References](#)

Original Paper:

Krassi Rumchev, Thet Win, Dean Bertolatti, and Satvinder Dhaliwal

Prevalence of respiratory symptoms among children in rural Myanmar-disease burden assessment attributable to household biomass smoke

Indoor and Built Environment 1420326X15586017, first published on May 20, 2015 as doi:10.1177/1420326X15586017

[Abstract](#) [Full Text \(PDF\)](#)  [References](#)

May 13, 2015

Original Paper:

Chanjuan Sun, Harry Giles, and Zhiwei Lian

Parametric regression model for lighting calibration

Indoor and Built Environment 1420326X15585859, first published on May 13, 2015 as doi:10.1177/1420326X15585859

[Abstract](#) [Full Text \(PDF\)](#)  [References](#)

Original Paper:

Xiaoli Wang and Angui Li

Airflow characteristics generated by fabric air dispersion ventilation

Indoor and Built Environment 1420326X15584424, first published on May 13, 2015 as doi:10.1177/1420326X15584424

[Abstract](#) [Full Text \(PDF\)](#)  [References](#)

May 8, 2015

Original Paper:

Li-Zhi Zhang, Rong-Rong Cai, and Jian-Chang Xu

Moisture transport through asymmetric porous membranes with finger-like holes for indoor humidity control: A lattice Boltzmann simulation approach

Indoor and Built Environment 1420326X15585326, first published on May 8, 2015 as doi:10.1177/1420326X15585326

[Abstract](#) [Full Text \(PDF\)](#)  [References](#)

May 6, 2015

Original Paper:

Kai Zhang, Xiaosong Zhang, Shuhong Li, and Xing Jin

Experimental parametric study on the temperature distribution of an underfloor air distribution (UFAD) system with grille diffusers

Indoor and Built Environment 1420326X15584805, first published on May 6, 2015 as doi:10.1177/1420326X15584805

[Abstract](#) [Full Text \(PDF\)](#)  [References](#)

Original Paper:

Qiong Wang, Yi Wang, Jingyuan Zhao, and Chunxia Bai

Diffusion factors of street canyon pollutants in the cold winter of Xi'an city based on back propagation neural network analysis

Indoor and Built Environment 1420326X15583918, first published on May 6, 2015 as doi:10.1177/1420326X15583918

[Abstract](#) [Full Text \(PDF\)](#)  [References](#)

April 23, 2015

Editorial:

Bob Giddings

The tyranny of energy conservation in the workplace

Indoor and Built Environment 1420326X15583422, first published on April 23, 2015 as doi:10.1177/1420326X15583422

[Full Text \(PDF\)](#)  [References](#)

April 20, 2015

Original Article:

Chan Lu, Qi-Hong Deng, and Chuck Wah Francis Yu

Strategies for reduction of episodic risk of PM₁₀ by controlling industrial and traffic emissions of SO₂ and NO₂ and meteorological parameters

Indoor and Built Environment 1420326X15581718, first published on April 20, 2015 as doi:10.1177/1420326X15581718

[Abstract](#) [Full Text \(PDF\)](#)  [References](#)

March 6, 2015

Original Paper:

Floriberta Binarti and Prasasto Satwiko

An east-facing anidolic daylighting system on a tropical urban house

Indoor and Built Environment 1420326X15574787, first published on March 6, 2015 as doi:10.1177/1420326X15574787

[Abstract](#) [Full Text \(PDF\)](#)  [References](#)

March 4, 2015

Original Paper:

Mirko Čudina, Jurij Prezelj, and Milena Pušlar-Čudina

The impact of paintings hung on lecture room walls on the speech intelligibility and perception of background noise

Indoor and Built Environment 1420326X15572640, first published on March 4, 2015 as doi:10.1177/1420326X15572640

[Abstract](#) [Full Text \(PDF\)](#)  [References](#)

February 27, 2015

Original Paper:

Hua Chen, Wai Ling Lee, and Ai-Xia Wu

Performance of a dry cooling and dedicated ventilation system under different operating conditions

Indoor and Built Environment 1420326X15574122, first published on February 27, 2015 as doi:10.1177/1420326X15574122

[Abstract](#) [Full Text \(PDF\)](#)  [References](#)

February 25, 2015

Original Paper:

Jorge S. Carlos

Simulation of the influence of an attic on the building energy efficiency in the Portuguese climate

Indoor and Built Environment 1420326X15573846, first published on February 25, 2015 as doi:10.1177/1420326X15573846

[Abstract](#) [Full Text \(PDF\)](#)  [References](#)

February 24, 2015

Original Paper:

Tahsin Yilmaz and Rifat Olgun

Investigation of the differences between factors affecting vandalism in urban green areas

Indoor and Built Environment 1420326X15573275, first published on February 24, 2015 as doi:10.1177/1420326X15573275

[Abstract](#) [Full Text \(PDF\)](#)  [References](#)

An east-facing anidolic daylighting system on a tropical urban house

Floriberta Binarti and Prasasto Satwiko

Abstract

Sustainable core daylighting is expected to provide comfortable and healthy daylight in dense urban areas. One system, an anidolic daylighting system is a promising solution, however, it is still not widespread because of several complications. This paper presents an application of an affordable anidolic daylighting system on a tropical urban house designed with a simple edge-ray approach. This approach has created a parabolic collector for east-facing (azimuth 85°) anidolic daylighting system to improve the daylighting level of a room with high external obstruction. Simulation results and short-term monitoring before and after the construction have indicated successful application of an anidolic daylighting system for improving daylighting performance, especially before 13:00, without increasing indoor air temperature. The results have shown a strong hourly illuminance profile. To improve the indoor illuminance after 13:00 and the hourly illuminance profile, an east-facing anidolic daylighting system collector can be combined with a west-facing collector.

Keywords

Anidolic daylighting system, Daylighting performance, Indoor air temperature, Monitoring, Simulation, Urban tropical house

Accepted: 3 February 2015

Introduction

A badly lit interior because of high external obstructions from the neighbourhood is a common problem in dense urban settlements. This study proposes an application of an affordable anidolic daylighting system (ADS) to improve the daylighting performance of a living room in a humid tropical urban house without increasing indoor air temperature.

An ADS was developed based on the edge-ray principle. ADS comprises of a parabolic collector, light transport medium and parabolic reflector as a light distributor at the end of the system.¹ An ADS prototype on a $5.4\text{ m} \times 3.4\text{ m} \times 2.7\text{ m}$ test room in Lausanne, Switzerland achieved outstanding daylighting performance without and with 40° external obstructions even under overcast sky conditions based on the monitoring of the illuminance and the daylighting autonomy. In this study, three novel anidolic systems: anidolic ceiling, integrated anidolic system and anidolic solar blinds, were presented as daylighting solutions for different specific location and condition.¹ Eight years later, Linhart and Scartezzini² assessed the ADS on the

LESO building on the EPFL campus in Lausanne considering occupant satisfaction, and suggested an energy-efficient, complimentary electric lighting system.

A prototype of an anidolic system in hot humid climates exists in Singapore, Bangkok in Thailand and Johor State, Malaysia. The highest sky luminance, which often occurs in the zenithal area in the tropics, benefits the system. Glare risk can be reduced by a shading effect on the room's windows. An anidolic integrated ceiling installed on a $6\text{ m} \times 6\text{ m} \times 2.75\text{ m}$ office room in Singapore could improve the illuminance ratio.³ Praditwattanakit et al.⁴ proposed an internal light shelf inside a 9-m wide room equipped with a south-facing ADS in Bangkok to improve excessive

Department of Architecture, University of Atma Jaya Yogyakarta, Yogyakarta, Indonesia

Corresponding author:

Floriberta Binarti, Department of Architecture, University of Atma Jaya Yogyakarta, Jl. Babarsari 44 Yogyakarta 55281, Indonesia.

Email: flo.binarti@gmail.com

daylight and the distribution because of high luminosity of the tropical sky. These studies prove that ADS is a promising technology in core daylighting. However, the application of this system to buildings is not widespread because of a lack of planning tools and guidelines that enable architects and engineers to easily adopt it.⁵ An affordable anidolic system is one solution to make the application widespread.

ADS application in building renovation in tropical urban areas faces additional challenges. One must consider comprehensive aspects including ADS daylighting performance, thermal impact and the integration to the building façade with a reasonable cost. In building renovation, the existing building plan and dense urban context could bring orientation restrictions for anidolic application. Research on anidolic performance related to building orientation in Johor resulted in a south-facing anidolic system for the most uniform illuminance distribution in Malaysia.⁶ Unfortunately, the recommendation was only based on a single-day field measurement (on 4 January) of 1:10 scale building model.

Using a simple edge-ray approach, an east-facing ADS design has been applied to improve the daylight level of a highly obstructed room in a tropical urban house. A simulation study was employed to assist the design process and to measure whether ADS daylighting performance had met the design parameters. Monitoring of ADS performance on an urban house was conducted to observe the real daylighting and thermal performance before and after ADS installation.

Methods

Application of the ADS in the renovation of a tropical urban house comprises two phases. The first phase is the design process, and it is followed by the monitoring phase. The design process intends to achieve a high-performance ADS exhibited by improvement of daylighting performance, minimal environmental impact and a good visual appearance. A simulation study was considered the most efficient design approach to predict ADS performance compared with a physical model relying on uncontrollable climatic conditions. One-year monitoring is conducted to assess the installation impacts on the indoor comfort and energy consumption for lighting. However, some indications could have been observed during short-term monitoring.

ADS model

Located in tropical medium-dense urban area in Yogyakarta, Indonesia, 7°49'27"S and 110°21'42"E, the living room is enclosed by a corridor on the east side, a terrace with high external obstruction from the

neighbouring building to the north, a bedroom on the west side and a kitchen on the south. These specifications had created a poorly lit interior in the living room (see Figure 1). Linhart et al.⁷ identified four influencing parameters of anidolic system in the tropics and listed them in ascending order as follows: surface coating, length, external shading and collector width. Collector orientation was not considered here, although under clear sky conditions, it may modify the daily or hourly daylighting performance (effective working time of the system). A study on ADS in Johor suggested a particular orientation for achieving the best performance.⁶ However, the only possible location for the collector in the present study is on the east or west façade. Compared with a west-facing collector, an east-facing collector shortens the light transport medium, which means less energy will be lost.

A 300-cm long, 40-cm high clerestory without glazing acting as the ADS opening corresponds to 9% of the window to floor area ratio. This possible installed area is smaller than the minimum requirement of 15%.⁸ Two clerestories installed on both corridor walls allow reflected sunlight and skylight to enter the living room through the corridor. The external clerestory should be installed at a position with a high vertical sky component (VSC) to harness optimum daylight without obstruction. In this case, the advantage of the light transport system of the ADS can be employed to improve the daylight level of a significantly externally obstructed room. VSC is the amount of direct skylight falling on a vertical plane. Whereas, the term of sky factor (SF) is used to describe the amount of direct skylight incident upon a plane with any tilt angle.⁹ The highest possible position of the clerestory creates 38.3% of VSC, which is close to the maximum VSC of 39.6%.

The geometry of ADS collector and reflector was designed based on the edge-ray principle. This principle is explained¹ as follows: (a) optical extent of the exiting lightflux equal to the incident flux, (b) minimum reflections of light rays in the transport medium and (c) high angular selectivity of the optical system design. After the parabolic height has been determined, the next step is to calculate the parabolic width or shape. Through the parabolic focal point, the shape should capture optimum daylight that would be reflected by the collector that travel through the light transport medium in parallel rays. To keep the indoor air temperature from increasing, the shape should exclude direct sunlight. ADS material was selected based on its surface reflectance, visual appearance and affordability. If light travels through the transport medium without any reflections, the energy quantity of the reflected light should be determined mainly by the collector surface reflectance.

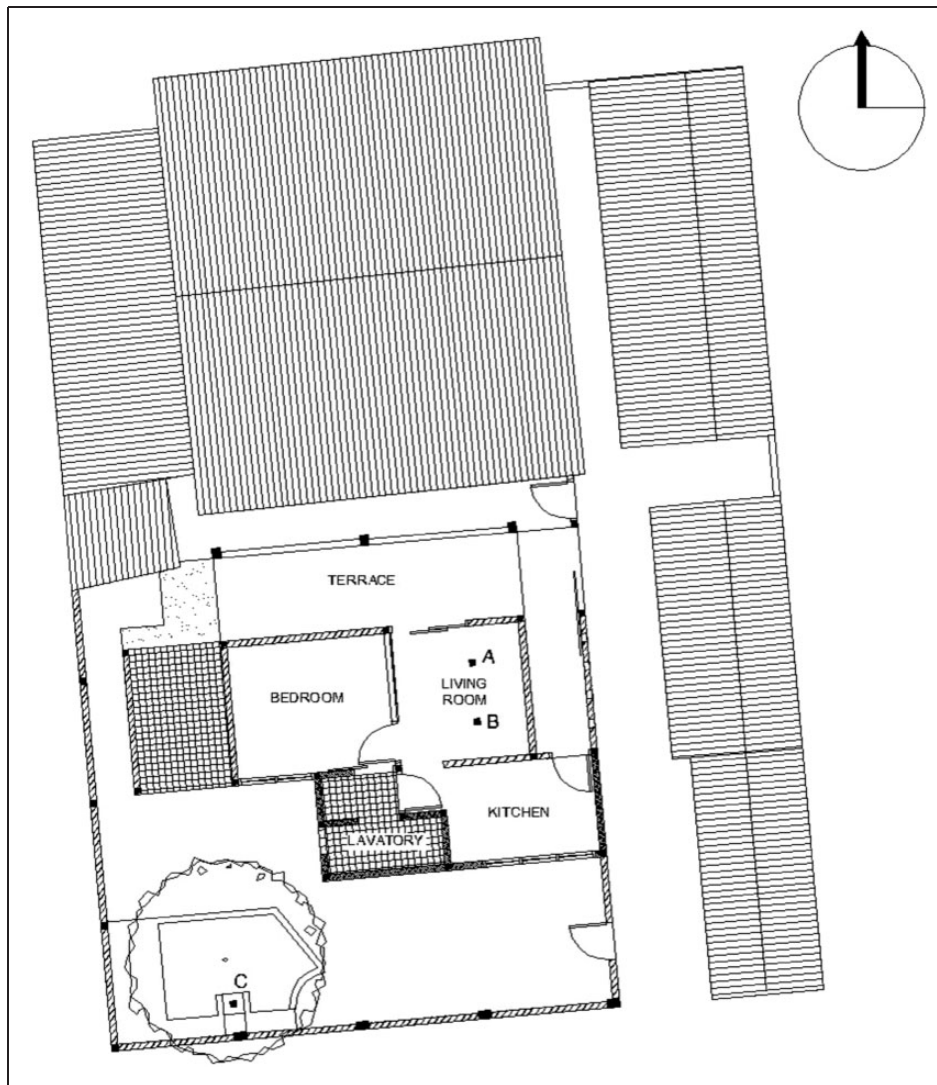


Figure 1. The house site plan with three positions (points A, B, and C) of the instruments.

Simulation study

A simulation study was conducted to estimate the ADS daylighting performance. The availability of a suitable sky luminance model is essential for daylighting simulation. A study on tropical sky luminance distribution conducted in Bangkok¹⁰ concluded that tropical sky is dominated by partly cloudy and clear skies. Overcast sky occurs 20% of a year. Linhart et al.⁷ presented four predominant sky types in Singapore with their relative occurrence as follows: Commission Internationale de l'Éclairage (CIE) standard overcast sky (33%), overcast sky (28%), partly cloudy sky (28%) and CIE standard clear sky (11%). Because of the lack of thorough studies on sky luminance in the specific location, sky luminance models used in the simulation study were based on other previous studies. Daylighting simulations

would be conducted under overcast and clear skies with the sun.

The daylighting performance of the ADS models was analysed using Radiance (plugged in Ecotect)^{11,12} and Aftab Alpha.¹³ Using a backwards ray-tracing algorithm, Radiance is recognised as a physically accurate daylighting program.¹⁴ The following four-sky types are available in radiance: sunny sky (CIE clear sky), intermediate sky, cloudy sky (CIE overcast sky), and uniform sky. CIE overcast sky represents the worst sky conditions, exactly at noon in mid winter,¹² which is commonly used to calculate the daylight factor (DF).

The DF (%) describes a ratio of daylight illumination at a specific point in a space to the simultaneous unobstructed outdoor illumination. Radiance (plugged in Ecotect) adopts the Building Research Establishment (BRE) split flux method¹² to calculate the DF of each

particular point defined in the grid area as the sum of three separate components of the natural light that reaches the points.¹² These three components are the sky component (SC), externally reflected component (ERC), and internally reflected component (IRC). This calculation is based on an assumption that ignores direct sunlight. SC is the portion of the natural light that directly enters through an opening. ERC is the percentage of the natural light reflected by any external elements outside the room or building. IRC can be calculated using equation (1):

$$\text{IRC} = \frac{0.85W}{A(1-p_1)}(Cp_2 + 5p_2) \quad (1)$$

W = window area (m^2), A = total internal surface area (m^2), C = coefficient of external obstructions, p_1 = area-weighted average reflectance of area A (using 0.1 as reflectance for glass), p_2 = average reflectance of surfaces below working plane, p_3 = average reflectance of surfaces above working plane.

Despite the accuracy of radiance that has been proven by several studies,^{14–16} two studies have disputed CIE overcast sky model. A deviation between the DF simulation and measurement was observed by Kleindienst¹⁴ because of the CIE overcast sky model and the DF method. Moreover, DF calculations under the CIE overcast sky model conducted in Hong Kong by Ng¹⁷ described 50% overestimation of the daylight availability when the angle of obstruction is high. These discrepancies can be understood because the CIE sky luminance distribution models used in the simulation program are idealised and uncommon, whereas the real sky is subtle and constantly changing.¹⁴

Ecotect v. 5.5 provides some options to increase the DF calculation accuracy. More accurate calculation options use the glazing refractive index to calculate the additional variable transparency of the glazing due on the angle of incidence of each ray. The increased accuracy option also uses the external reflectance value calculated from the colour of each external obstruction in the ERC calculation. This method also impacts the contribution of each ray in the SC calculation, which could be moderated by the transparency of each window. Specific glazing transparency and specular value could provide more realistic internal reflections for each glass.¹²

Daylighting simulations were setup with high calculation accuracy and four indirect reflections. Instant maps were simulated to visualise the illuminance on the June solstice (June 21 at 12:00 to represent the DF and at 16:00, the worst sky conditions), October 15 at 11:00 (the highest altitude) and March 21 at 11:00, or the March equinox. The average six-day

field measurements of the DF and the indoor illuminance (E_i) were used to calibrate the internal surface reflectance of the existing building.

Aftab Alpha, Evalglare¹⁸-based software, was employed to analyse the glare of illuminance or luminance pictures created by radiance. The goal of the ADS application is to create a pleasant interior with at least 50 lux of the illuminance, 1% of the DF¹⁹ and to maintain the daylight glare index probability (DGP) with an imperceptible glare <30%.²⁰ DGP is a glare rating derived from subjective user evaluations inside lit rooms. DGP is considered the most robust metric and least prone to produce inaccurate glare predictions because it considers the most factors that contributes to visual discomfort.²¹ The DGP is defined by equation (2)²⁰

$$\text{DGP} = 5.87 * 10^{-5} E_v + 9.18 * 10^{-2} \left(1 + \sum_j \frac{L_{s,j} * \omega_{s,j}}{E_v^{1.87} * P_j^2} \right) + 0.16 \quad (2)$$

E_v = vertical illuminance at the eye, L_s = luminance of the glare source, ω_s = solid angle of the source, P = position index of the source.

Monitoring

Short-term monitoring covers field measurements of the indoor and outdoor illuminance, air temperature, relative humidity (RH), the ambient illuminance on a horizontal plane (E_{amb}) and its DGP. Monitoring of the indoor climate (illuminance level, air temperature and RH) was conducted for two different location points on the north–south axis of the room named point A and point B (see Figure 1). These two points represent the entire workplan of the 3.3-m wide living room. Indoor illuminance (E_i), air temperature (T_i) and RH_i were monitored using two analogue 4-in-1 environment testers, the LM-8000 (its accuracy is 5% for light intensity, 1% for air temperature and 1.2–4% for RH), placed at seat height in the middle of the living room. Outdoor illuminance (E_o), air temperature (T_o) and RH_o measurements were conducted using the Luxmeter LX-107 (the accuracy is 5%) and a 4-in-1 environment tester, the LM-8000. These instruments were located around the house under the relatively constant shading of a tree (point C in Figure 1). Illuminance of a point below constant shading under clear sky conditions represents outdoor illuminance under overcast sky conditions. The sun path facility in Ecotect software was employed to examine the shading consistency during measurement. Digital equipments, a Hobo datalogger U12-012 for the indoor measurement and a Hobo datalogger UA 002-08 for

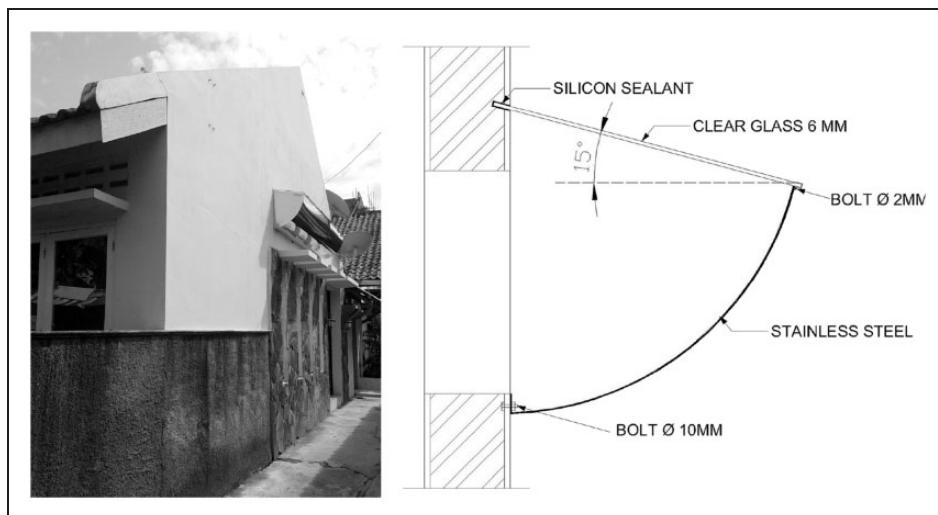


Figure 3. Photo of the east-facing ADS (left) and the detail of ADS collector (right).

Table 1. Daylighting performance of the living room based on simulations.

| Date, time, and sky condition | ADS type | DF (%) | | E_i (lux) | | DGP (%) |
|--|-------------------|--------|------|-----------------|-----------------|-------------------|
| | | A | B | A | B | |
| CIE overcast sky | Existing (no ADS) | 0.72 | 0.75 | 26 ^a | 23 ^a | 3.9 ^a |
| | 40-cm wide | 1.01 | 1.03 | 60 ^a | 61 ^a | 16.4 ^a |
| 21 June at 16:00 CIE overcast sky | Existing (no ADS) | | | 14 | 13 | 1.4 |
| | 40-cm wide | | | 34 | 35 | 6.7 |
| 15 October at 11:00 CIE clear sky with sun | Existing (no ADS) | | | 86 | 79 | 19.7 |
| | 40-cm wide | | | 364 | 369 | 26.0 |
| 21 March at 11:00 CIE clear sky with sun | Existing (no ADS) | | | 72 | 68 | 19.0 |
| | 40-cm wide | | | 336 | 355 | 25.6 |

Note: ADS, anidolic daylighting system; DF, daylight factor; DGP, daylight glare index probability.

^a21 June at 12:00.

façade, but still catches zenithal light from 10:00 until approximately 13:00. Morning daylight beams from 07:00 to 10:00 would be reflected on the pure white surface of the ceiling below the collector. The 2.58 m high and 1.5-m wide ceiling suspended below the collector (Figure 2(a)) would prevent uncomfortable glare from the collector (>2 m in height).

The ADS model was then developed using a stainless steel sheet as the collector material and painted pure white gypsum as the interior reflector material. Stainless steel was selected because of its availability, flexibility and high reflectance ($\rho_r = 0.9$). Moreover, this material can stand alone without additional material to support its weight or to improve the façade appearance (see Figure 3). Six-mm thick clear glass covers the parabolic collector with 15° of the tilt angle (Figure 2(b)) for rainfall run off and high-altitude daylight admission.

Simulation-based ADS performance

Simulation results reported that the 40-cm wide ADS improves the daylighting performance significantly even under the worst sky conditions, i.e. on 21 June at 16:00 under overcast skies. The DF increased approximately 39%, whereas the E_i increased approximately 150% under overcast sky conditions and 370% under a clear sky with the sun. Sufficient daylighting performance could be achieved with slightly higher than 1% of the DF and an imperceptible glare at the eye level of a seated person (DGP < 30%). On 21 June at 16:00, the illuminance levels of the house with ADS were below 50 lux. However, 34–35 lux would be a substantial improvement compared with the illuminance of the existing room at 16:00, i.e. 13–14 lux (Table 1).

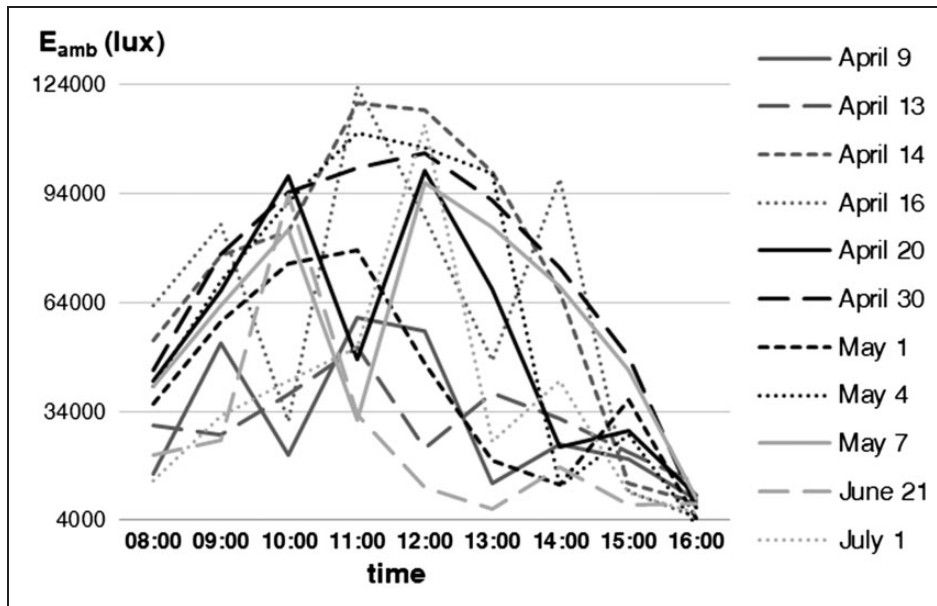


Figure 4. Ambient illuminance on a horizontal plane (E_{amb}) during monitoring, before installation: 9–20 April, after installation: 30 April–1 July.

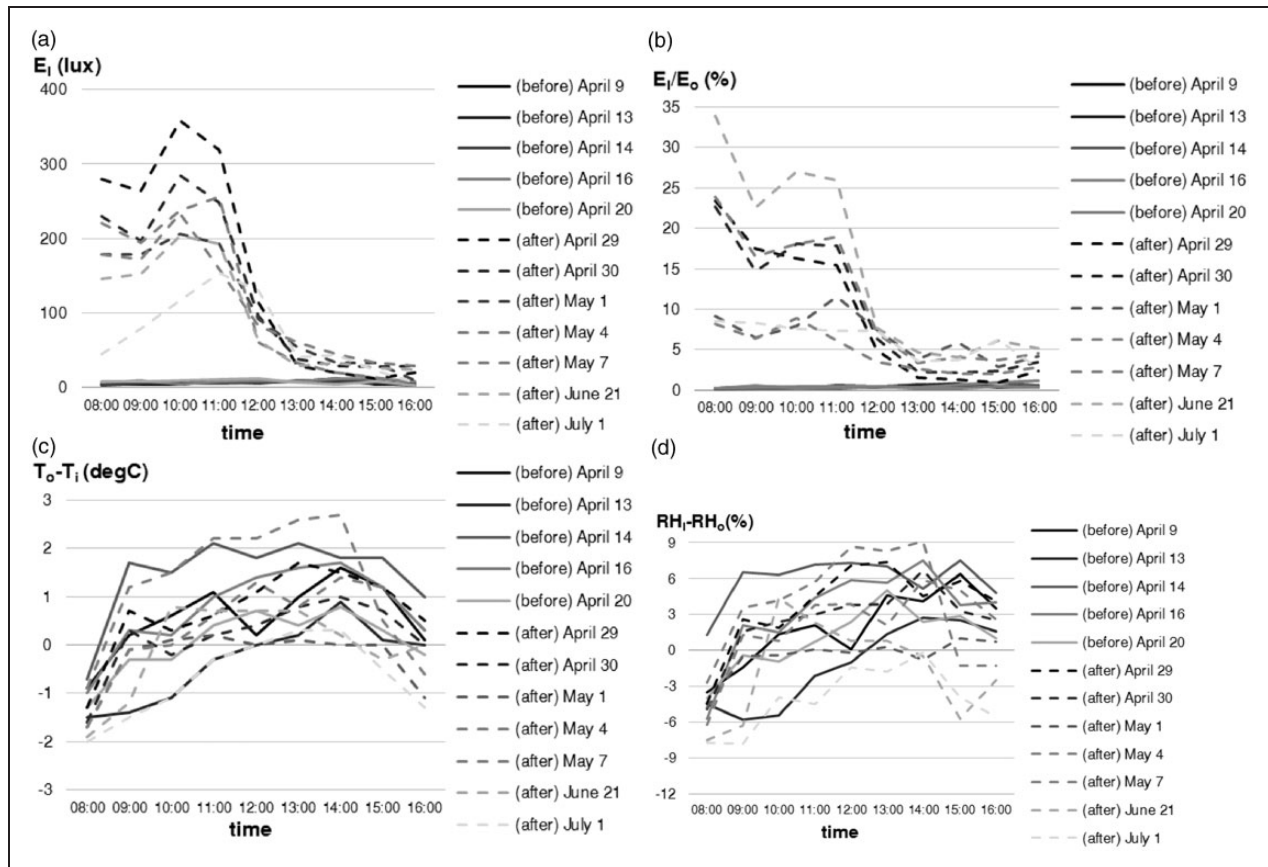


Figure 5. The E_i at point A (a), the E_i/E_o at point A (b), the $T_o - T_i$ at point A (c), and the $RH_i - RH_o$ at point A (d) of the living room before (before) and after (after) ADS construction.

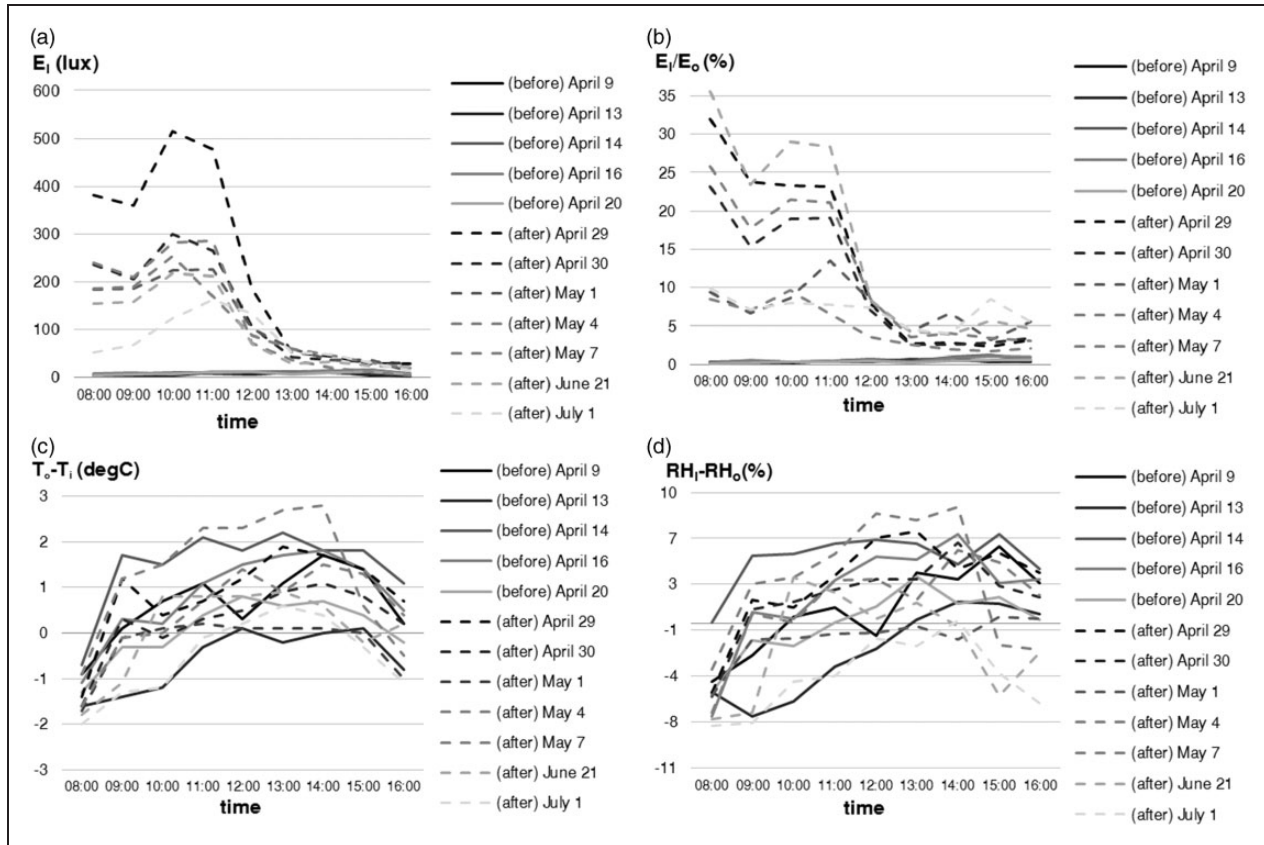


Figure 6. The E_i at point B (a), the E_i/E_o at point B (b), the $T_o - T_i$ at point B (c), and the $RH_i - RH_o$ at point B (d) of the living room before (before) and after (after) ADS construction.

Table 2. Results of the paired t -test.

| Thermal components | Number of data | Correlation | Significance | M | Standard error | Significance (two-tailed) or p value |
|--------------------|----------------|-------------|--------------|--------|----------------|--|
| $T_o - T_i$ | 90 | 0.889 | 0.000 | -0.589 | 0.055 | 0.289 |
| $RH_i - RH_o$ | 90 | 0.589 | 0.000 | 0.815 | 0.387 | 0.038 |

Note: RH, relative humidity.

When the sun was located at the longest distance from the ADS under overcast sky conditions, the E_i could reach more than 50 lux. Despite high sky illuminance on 15 October at 11:00, the DGP was still below 30%.

Monitoring-based ADS performance

The 40-cm wide ADS was constructed to study the effects of the edge-ray principle on real daylighting and thermal performance. Post ADS construction monitoring was conducted from the end of April to the beginning of July when the sky luminance was

lower than the annual one. Seventy-five percent of the monitoring measurements were taken under a clear sky with the sun and the remaining measurements were obtained under overcast and partly cloudy skies (see Figure 4).

The monitoring results show that the ADS installation improves the illuminance of the living room during the daytime without increasing the indoor air temperature and the RH (see Figures 5 and 6). Some diffuse morning sunlight from low altitude, directly falling on the parabolic reflector, produced high illuminance at 08:00. This results made the daylight levels at 08:00 higher than those at 09:00. Because solar radiation at



Figure 7. The glare analysis of the simulated interior with 20.4% for the DGP (left), HDR fisheye photo of the interior (middle), and the glare analysis of the real interior with 16.0% for the DGP (right) on 16 August at 11:00.

Table 3. Discrepancies between the measured and simulated illuminance of the living room with ADS on 30 April.

| Local time | Measured (1) | | Simulated (2) | | Discrepancy [(1-2)/1] | | |
|--------------------|--------------|-----|---------------|-----|-----------------------|-------|---------|
| | A | B | A | B | A | B | Average |
| 08:00 | 230 | 235 | 236 | 251 | -0.03 | -0.07 | -0.05 |
| 09:00 | 197 | 206 | 163 | 184 | 0.17 | 0.11 | 0.14 |
| 10:00 | 285 | 299 | 296 | 311 | -0.04 | -0.04 | -0.04 |
| 11:00 | 248 | 265 | 222 | 257 | 0.10 | 0.03 | 0.07 |
| 12:00 | 95 | 105 | 90 | 104 | 0.05 | 0.01 | 0.03 |
| 13:00 | 38 | 42 | 31 | 39 | 0.18 | 0.07 | 0.13 |
| 14:00 | 29 | 35 | 30 | 35 | -0.03 | 0.00 | -0.02 |
| 15:00 ^a | 27 | 31 | 30 | 30 | -0.11 | 0.03 | -0.04 |
| 16:00 ^b | 28 | 28 | 25 | 26 | 0.11 | 0.07 | 0.09 |

Note: ADS, anidolic daylighting system.

^aUnder intermediate sky with sun.

^bUnder overcast sky. No sign (): under clear sky with sun.

Table 4. Simulated DGP and measured DGP on August 16.

| Local time | DGP (%) | | |
|------------|------------|-------------|-----------------|
| | Simulation | Measurement | Discrepancy (%) |
| 10:00 | 20.7 | 15.7 | -24.0 |
| 10:30 | 20.5 | 15.4 | -25.0 |
| 11:00 | 20.4 | 16.0 | -22.0 |
| Average | | | -23.5 |

Note: DGP, daylight glare index probability.

08:00 was not high, this light did not increase the indoor air temperature. A combination of high indoor illuminance and low ambient illuminance at 08:00 even created the highest E_i/E_o . These conditions occurred intensely from April to June. On 21 June and 1 July, the hourly profiles of E_i/E_o appeared more flat because

some parts of the house covered the measurement location of E_o in the afternoon.

The highest illuminance was achieved at 10:00. At this time, the ADS collected more daylight that was then reflected to the living room. Although the ambient illuminance at 11:00 and 12:00 (see Figure 4) achieved the highest level, the daylight levels at these times were lower because of the lower daylight captured by the collector. The ADS would effectively work as a non-imaging collector from approximately 10:00 until 13:00 (see Figures 5 and 6). After this time, the collector reflects only diffuse daylight, which would improve the indoor illuminance and DF under clear sky conditions. Low illuminance (<50 lux) occurred after 13:00 and especially under cloudy skies on 21 June (see Figures 5 and 6).

Figure 5 (c) and (d) and Figure 6 (c) and (d) show that the air temperature and RH difference after installation (dashed line) were still in the same range as the

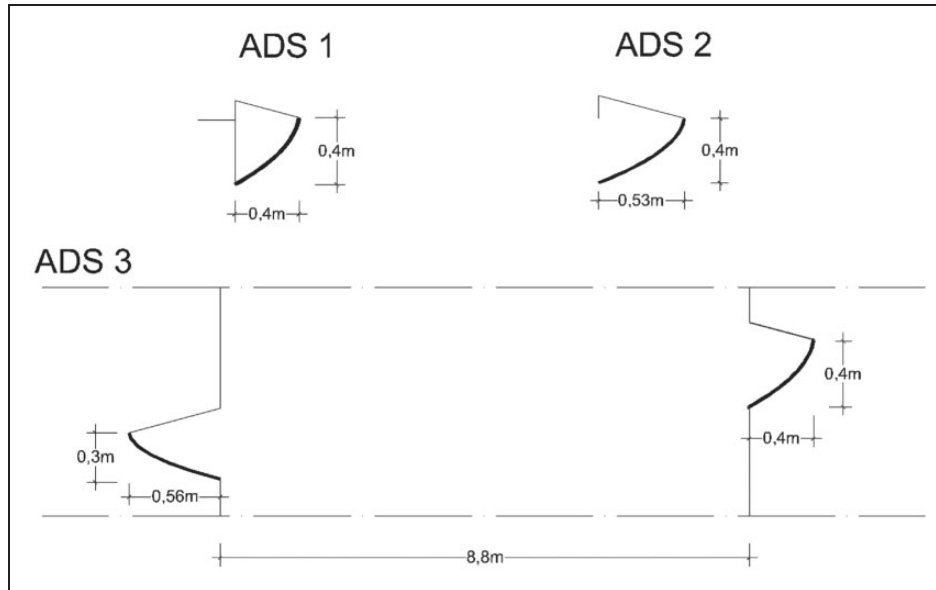


Figure 8. ADS models.

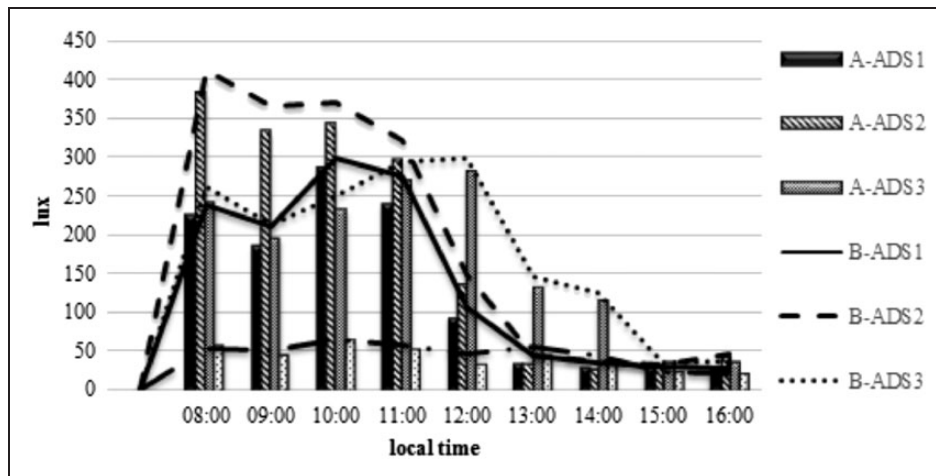


Figure 9. Calibrated simulation results of the illuminance at points A and B of three ADS models on 30 April.

Table 5. Simulated DGP and DF of 3 ADS models.

| ADS model | DGP (%) on 15 October at 11:00 | DF (%) | |
|-----------|--------------------------------|--------|------|
| | | A | B |
| ADS 1 | 27.1 | 1.01 | 1.03 |
| ADS 2 | 28.0 | 1.09 | 1.14 |
| ADS 3 | 19.3 | 1.00 | 1.05 |

Note: DF, daylight factor; DGP, daylight glare index probability; ADS, anidolic daylighting system.

air temperature and RH difference before installation (straight line). Table 2 shows that the temperature difference ($T_o - T_i$) before ADS installation had a strong

(the correlation is close to 1) and significant correlation with $T_o - T_i$ after ADS installation. The p value (>0.05) and the mean indoor air temperature difference (0.589°C) confirmed that the ADS installation did not modify the indoor air temperature. Null of significance means that the correlation was significant at the level of 0.05.

The paired t -test of the air humidity difference ($\text{RH}_i - \text{RH}_o$) was rather different. There was insignificant correlation between the $\text{RH}_i - \text{RH}_o$ measured before and after ADS installation demonstrated by the low correlation (0.589). The p value (<0.05) and the mean (0.815%) have illustrated there was a small difference in the RH because of the ADS installation.

By tracing the outdoor and indoor air humidity measured before and after ADS installation (see Figures 5 and 6), the low p value could be explained by a combination of very low outdoor air humidity with high indoor air humidity that occurred on 4 May and 1 July. Exceptionally small activity conducted inside the house during that day could have increased the moisture content.

The reported DGP measurement that reflected daylight from the collector would create a comfortable indoor illuminance at eye level. The DGP on 16 August at 11:00, when the ambient horizontal illuminance reached 106,900 lux and the indoor illuminance was 247 lux, was only 16% (see Figure 7 and Table 4). This ambient horizontal illuminance and indoor illuminance on that day are considered being high compared with the illuminances on other days (see Figures 4–6).

Between simulation and monitoring of the ADS performance

The simulation-based DF of the living room with ADS was slightly greater than 1%. This result is much different from the field measurements. The average E_i/E_o measured on the June solstice under overcast sky conditions with the ambience illuminance (E_{sky}) at approximately 7233–13,089 lux could reach 6.3%, whereas the E_i/E_{amb} at the same time was only 0.45%. The E_i difference between the simulation and measurement results on 21 June at 16:00 confirms the accuracy of the CIE overcast sky. A discrepancy in E_i on 21 June at 16:00 was 50% and at 12:00 under clear sky with the sun, the discrepancy was only 8%.

To simulate the regular pattern of a naturally luminous environment in order to find accurate results, this study used discrepancy values as a percentage of differences between the measurement results and the simulations that were performed hourly (from 08:00 to 16:00) under a representative CIE sky condition at that time to describe the ADS performance, which was close to the real condition. 30 April was selected because of the most regular hourly profile of the ambient illuminance (see Figure 4).

A discrepancy of the measurement and simulation results signifies a consequence to the difference between real and simulated DGP on 16 August (Table 4). During that time, the indoor illuminance could reach 225 lux at 10:00, 242 lux at 10:30 and 247 lux at 11:00. Monitoring and simulations of the illuminance on 16 August from 10:00 to 11:00 confirmed that simulations of the indoor illuminance under a clear sky with the sun with four indirect reflections were 15% higher than the measured conditions. Furthermore, the simulated DGP could be calibrated using the average discrepancy of the

real and simulated DGP on 16 August, or –23.5%. By using this value, the calibrated simulation DGP on 15 October at 11:00 was only 20%.

Modifications of the east-facing ADS

Although the discrepancy between the simulation and field measurements varies, the overall simulations and monitoring of the 40-cm wide ADS application have confirmed that this system could improve the daylighting performance of the living room. To improve the indoor illuminance after 13:00, the collector shape was modified into three ADS models (see Figure 8). The first alternative could lengthen the distance of the focal point from the façade wall to capture more daylight in the afternoon. This alternative had resulted in a 53-cm wide ADS collecting sun beam from 09:00 to 13:00 (ADS 2). The second alternative added a collector on the west façade to catch afternoon daylight. Daylighting performances of the modified ADS were simulated on 30 April (the date was selected in 3.2), which was calibrated using the average discrepancy values in Table 3.

Figure 9 and Table 5 describe the daylighting performances of all ADS models on 30 April. The 53-cm wide ADS had created the highest indoor illuminance before 12:00 and surprisingly at 16:00. A simulation result of this model reported that the average DF was 1.1%, and the DGP on 15 October at 11:00 was 28%. ADS with double-facing collectors could improve indoor illuminance in the afternoon under a clear sky with sun. The DF was 1.0% and the DGP was 19.3%.

Conclusions

Simulation and monitoring results have confirmed that the ADS application could be a promising solution for daylighting problems in tropical regions. ADS could offer an opportunity for buildings in a highly dense urban area to catch direct and diffuse sunlight with higher SF than the SF of a vertical window on the same height. Even during the worst conditions in the southern hemisphere of tropical regions for east-facing ADS (in the June solstice), the east-facing ADS could still have resulted in significant improvement in the daylighting performance without any influences on the indoor air temperature. The white bright space created by ADS installation with proper geometrical features provides a more pleasant atmosphere, but still maintain imperceptible glare. However, a strong hourly illuminance profile was performed by the east-facing ADS. To improve the low illuminance produced by the east-facing ADS after 13:00, west-facing collector with a proper shape may be added. The overall results proved that the conventional approach in determining

the opening dimension (daylighting rule of thumb) can no longer be adopted in this advanced daylighting system. A new rule for this system is needed as a design guideline for more widespread applications.

Authors' contribution

This research was conducted by the first author and supported by the coauthor as the research advisor and manuscript proofreader.

Declaration of conflicting interests

The authors declared no potential conflicts of interest with respect to the research, authorship, and/or publication of this article.

Funding

This research was financially supported by Directorate of Higher Education, Ministry of National Education and Culture of Republic Indonesia for the research grant in the scheme of "Competitive Grant" (*Hibah Bersaing*) under the project "Model and rule of thumb of the integrated daylighting system for creating environmentally friendly interior" with contract numbers: 1317/K5/KM/2014 (Government to University) and 006/SP-HB/II/2014 (University to Researcher).

References

- Scartezini JL and Courret G. Anidolic daylighting systems. *J Sol Energy* 2002; 73: 123–135.
- Linhart F and Scartezini JL. Minimizing lighting power density in office rooms equipped with anidolic daylighting systems. *J Sol Energy* 2010; 84: 587–595.
- Wittkopf SK. Daylight performance of anidolic ceiling under different sky conditions. *J Sol Energy* 2006; 81: 151–161.
- Praditwattanakit R, Chaiwiwatworakul P and Chirarattananon S. Anidolic concentrator to enhance the daylight use in tropical buildings. In: *International Conference on Alternative Energy in Developing Countries and Emerging Economies*. Bangkok, 30–31 May, ftp://202.28.64.61/04.April2013/Download/print/139_Rut%20Praditwattanakit.docx (2013, accessed 7 August, 2014).
- Wittkopf SK, Grobe LO, Compagnon R, Kampf J, Linhart F and Scartezini JL. Ray tracing study for non-imaging daylight collectors. *J Sol Energy* 2010; 84: 986–996.
- Roshan M, Kandar MZB, Nikpur M, Mohammadi MP and Ghasemi M. Investigating the performance of anidolic daylighting system with respect to building orientation in tropical area. *IRACST-ESTIJ* 2013; 3: 74–79.
- Linhart F, Wittkopf SK and Scartezini JL. Performance of anidolic daylighting systems in tropical climates—parametric studies for identification of main influencing factors. *J Sol Energy* 2010; 84: 1085–1094.
- Leadership in Energy and Environmental Design (LEED). *Reference guide for green building design and construction, for the design, construction and major renovations of commercial and institutional building including core and shell K-12 school projects*, www.usgbc.org (2009, accessed 6 November, 2010).
- Andersen M. Generalization of the direct sky component calculation to openings of arbitrary tilt angle. *LEUKOS—J IESNA* 2004; 1: 39–55.
- Chirarattananon S and Chaiwiwatworakul P. Distribution of sky luminance and radiance of North Bangkok under standard distributions. *J Renew Energy* 2007; 26: 1328–1345.
- Ward G. *Desktop radiance software*. Berkeley, CA: Lawrence Berkeley Laboratory, 2002.
- Marsch A. Ecotect software v.5.5. Square One, Cardiff, 2005.
- Miri M. Aftab Alpha software v.1.1.0, http://aftabsoft.net/AftabAlpha/Software/Aftab_Setup.exe (accessed 24 February, 2014).
- Kleindienst SA. *Improving the daylighting conditions of existing buildings: the benefits and limitations of integrating anidolic daylighting systems using the American classroom as a model*. Master thesis. Massachusetts Institute of Technology, Massachusetts, 2006.
- Lim YW, Ahmad MH and Ossen DR. Empirical validation of daylight simulation tool with physical model measurement. *Am J Appl Sci* 2010; 7: 1426–1431. ISSN 1546-9239.
- Yi R, Shao L, Su Y and Riffat S. Daylighting performance of atriums in subtropical climate. *Int J Low-Carbon Technol* 2009; 4: 230–237.
- Ng E. A study on the accuracy of daylighting simulation of heavily obstructed buildings in Hong Kong. In *Proceedings of 7th International IBPSA Conference*, Rio de Janeiro, 13–15 August, 2001, pp. 1215–1222.
- Wienold J. *Evalglare software*. Freiburg, Germany: Fraunhofer Institute for Solar Energy System, 2005.
- Illuminating Engineering Society. *IES lighting handbook*. 10th ed. New York: Illuminating Engineering Society (IES), 2011.
- Wienold J. Evaluation methods and development of a new glare prediction model for daylight environment with the use of CCD cameras. *J Energy Build* 2006; 38: 743–757.
- Jackubiec JA and Reinhart C. The 'adaptive zone'—a concept for assessing discomfort glare throughout daylit spaces. *Light Res Technol* 2012; 44: 149–170. DOI: 10.1177/1477153511420097.
- Ward G. *Photosphere for Mac*. Los Angeles, CA: Anywhere software, 2003.